



Prehistoric agricultural practices and subsistence strategies at Jicha site (3800–2200 cal BP) in Northwest Yunnan, China

Xiabo Li ^a , Wuqi Zhang ^{a,b}, Qing Yang ^{a,b,*} , Changcheng Hu ^c, Nan Cheng ^b, Jie Fu ^d , Zining Zou ^a , Yuanyuan Gao ^e , Hongbo Zheng ^{f,g}

^a Yunnan Key Laboratory of Earth System Science, Yunnan University, Kunming 650093, China

^b Key Laboratory of Digital Human Technology R&D and Application of Yunnan Provincial Department of Education, School of History and Archival Science, Yunnan University, Kunming 650032, China

^c Yunnan Institute of Cultural Relics and Archaeology, Kunming 650118, China

^d School of Archaeology and Museology, Sichuan University, Chengdu 610207, China

^e School of History and Culture (School of Tourism), Southwest Minzu University, Chengdu 610041, China

^f Sustainable Minerals Institute, University of Queensland, Brisbane, QLD 4068, Australia

^g Australian Research Centre for Human Evolution, Griffith University, Brisbane, QLD 4111, Australia

ARTICLE INFO

Keywords:

Northwest Yunnan
Late Neolithic to Bronze Age
Jicha site
Phytolith analysis
Subsistence strategy

ABSTRACT

Northwest Yunnan, historically a pivotal corridor for interactions among various ethnic groups from northern and southwestern China, played a significant role in prehistoric human migrations and the dissemination of agriculture. The Jicha site, located at the south end of the Hengduan Mountains in northwest Yunnan, is an important metallurgical site occupied during the period from the Late Neolithic to the Early Iron Age. Based on phytolith analysis of soil samples collected from this site, this study reveals that the inhabitants from 3800 to 2200 cal BP primarily subsisted on cultivated plants. Within the relatively stable agricultural system, rice remained the staple diet, complemented by dryland crops such as wheat, foxtail millet, and common millet. Among these crops, wheat appeared around 3500 cal BP and became the dominant dryland crop by the Middle to Late Bronze Age. Additionally, the inhabitants diversified their diet by utilizing plant resources effectively from the surrounding areas. The evidence indicates the ancestors had an advanced capacity to organize social labor and developed relatively mature skills for cultivation management and crop processing, which were related to large-scale grain harvesting and processing or storing in specific areas and possibly further strengthened rice cultivation.

1. Introduction

The Hengduan Mountains region in southwestern China, located at the transitional zone between the Qinghai-Tibet Plateau and the Yunnan-Guizhou Plateau, has served as a transcontinental crossroads for millennia. This area, ethnographically termed the “Tibetan-Yi Corridor”, has facilitated population migrations and cultural exchanges among East, Southeast, and South Asian communities, hosting settlements of Tibetan, Han, and Yi ethnic groups renowned for their ethnic diversity, cultural complexity, and well-preserved archaeological heritage (Shi, 2009). As a critical locus for the origin, differentiation, and integration of Tibetan-Yi populations, the region also holds significance for studying interethnic cultural interactions. Archaeological evidence underscores

the eastern Tibetan Plateau as a major corridor for southward migrations of ancient populations from northwestern China’s Gansu-Qinghai region (Huo and Ren, 2022; Li, 2020; Shi, 2009). Northwestern Yunnan, as the southern extension of this corridor, features the “Three Parallel Rivers” geomorphology—comprising the Jinsha, Lancang, and Salween River valleys—which connect the Qinghai-Tibet Plateau with Southeast Asia. Despite its archaeological potential, rugged topography has impeded preservation of prehistoric remains, leaving gaps in understanding early population movements and cultural exchanges. Recent systematic surveys by the Yunnan Provincial Institute of Cultural Relics and Archaeology have identified key Neolithic to Iron Age sites, including the 2022-excavated Jicha site (Fu et al., 2024). This metallurgical settlement, spanning the Late Neolithic to Iron Age, reveals

* Corresponding author.

E-mail address: yangqing@ynu.edu.cn (Q. Yang).

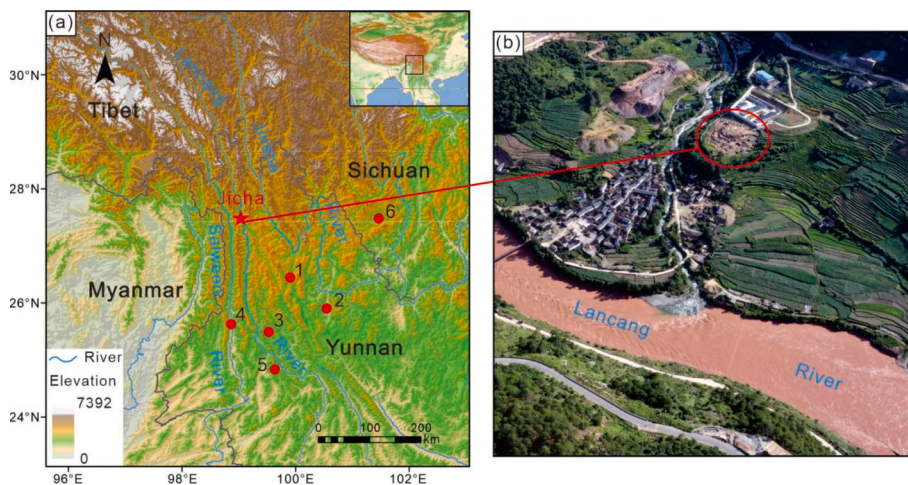


Fig. 1. (a) Location of the Jicha site (red star) and other sites mentioned in the study (red dots): (1) Haimenkou, (2) Baiyangcun, (3) Xinguang, (4) Shilinggang, (5) Yingpanshan, (6) Guijiabao. (b) Aerial view of the Jicha site.

pottery motifs in its Late Neolithic layers strikingly similar to those at upstream Karuo and downstream Haimenkou sites along the Lancang River, indicating regional cultural networks.

The Jicha site's strategic position offers critical data for reconstructing prehistoric cultural dynamics and agricultural diffusion along the Hengduan Mountains' north–south corridor. Prehistoric agriculture in Yunnan has been preliminarily framed through macro-botanical studies, with Li et al. (2016) proposing three developmental stages: rice-dominated agriculture (4800–3900 cal BP), mixed rice-millet systems (3900–3400 cal BP), and diversified crops (rice, millet, wheat/barley; 3400–2300 cal BP). Dal Martello et al. (2018, 2021) challenged this chronology, arguing for coexisting rice and millet cultivation as early as 4600 cal BP and refining the timeline into three phases: mixed rice-millet farming in the 3rd millennium BC, wheat/barley introduction in the 2nd millennium BC, and a diversified system centered on northwestern Yunnan's Baiyangcun and central Yunnan's Dianchi regions during the 1st millennium BC (Dal Martello, 2022). However, regional and temporal variations in agricultural trajectories remain understudied due to limited archaeobotanical research, particularly from the Late Neolithic to the Bronze Age. This gap stems from restricted fieldwork and Yunnan's acidic soils, leading to the deterioration of macrobotanical evidence.

Phytolith analysis, a robust method for reconstructing ancient diets and agricultural systems (Lu et al., 2009a, 2009b; Weisskopf et al., 2015a; Zhang et al., 2010, 2024; Zuo et al., 2017), offers a solution. Unlike macrobotanical remains, phytoliths resist acidic conditions, preserving even in Yunnan's challenging soil environments. Despite its potential, phytolith analysis remains underutilized in Yunnan, with only limited applications at sites like Dayingzhuang (Dal Martello, 2022), Xueshan (Wang et al., 2022), Xiaodong Rockshelter (Wang, 2022), and Shilinggang (Li et al., 2016).

This study applied phytolith analysis to the Jicha site's Late Neolithic to Iron Age layers, complemented by AMS radiocarbon dating and stratigraphic phasing. Diatom species were also examined to contextualize environmental conditions. This study investigates the agricultural patterns and plant resource utilization strategies at the site, addressing a critical gap in the prehistoric agricultural chronology of Yunnan. The findings establish a scientific foundation for exploring prehistoric human migration, agricultural dispersal, and cultural evolution in northwestern Yunnan.

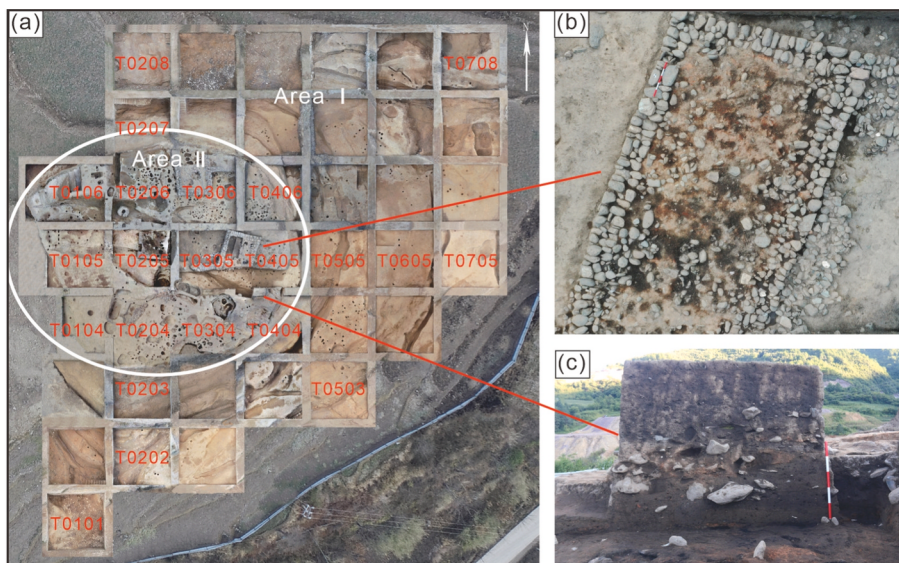


Fig. 2. (a) Schematic diagram of the excavation area at the Jicha site. (b) Core area house site. (c) Wall section of excavation unit T0405.

Table 1AMS¹⁴C Dating Results for Remains in Area II of Jicha site (Fu et al., 2024).

Lab No.	Sample No.	Material	Archaeological Phase	Radiocarbon age range (BP, 2σ)	Calibrated Age (cal BP)
Beta-649809	2022WJM50	Bone	Phase IV	2230 ± 30	2272–2149
Beta-649805	2022WJM11	Bone	Phase IV	2410 ± 30	2499–2348
Beta-649807	2022WJF4②	Rice	Phase IV	2440 ± 30	2540–2357
Beta-649804	2022WJY5	Wheat	Phase IV	2440 ± 30	2540–2357
Beta-649808	2022WJL2	Charcoal	Phase III	2950 ± 30	3209–3000
Beta-649811	2022WJM31	Bone	Phase III	2420 ± 30	2515–2351
Beta-649806	2022WJM12	Bone	Phase III	2450 ± 30	2544–2361
Beta-649812	2022WJM35	Bone	Phase III	2490 ± 30	2724–2463
Beta-649814	2022WJM46	Bone	Phase III	2500 ± 30	2727–2487
Beta-649810	2022WJF15ZC	Seeds	Phase III	2500 ± 30	2727–2487
Beta-649815	2022WJL10	Rice	Phase II	3100 ± 30	3383–3227
Beta-643098	2022WJH112	Charcoal	Phase II	3100 ± 30	3383–3227
Beta-649817	2022WJHDM5	Rice	Phase II	3250 ± 30	3512–3391
Beta-649816	2022WJG29	Bone	Phase II	3310 ± 30	3583–3453
Beta-649818	2022WJT0405⑨	Rice	Phase II	3300 ± 30	3578–3450
Beta-649813	2022WJG17④	Rice	Phase I	3480 ± 30	3837–3687

2. Materials and methods

2.1. Overview of the study area

The Jicha site ($27^{\circ}20'19.73''\text{N}$, $99^{\circ}05'22.47''\text{E}$) is located in Weixi Lisu Autonomous County, Diqing Tibetan Autonomous Prefecture, Yunnan Province (Fig. 1a). It is situated in the southeastern part of the Qinghai-Tibet Plateau, specifically within the mid-section valley belt of the Hengduan Mountains and lies within the Lancang River Basin, which is part of the “Three Parallel Rivers” World Natural Heritage area. The region has an average elevation of 2340 m. The topography is rugged, featuring steep slopes and deep valleys that descend from north to south. Climatic records show the area has an annual mean temperature of 14.7°C and an annual precipitation of 1121.6 mm.

The site is located on a secondary terrace (elevation: ca. 1700 m) at the confluence of the west bank of the Lancang River and the north bank of the Jicha River (Fig. 1b). Before the construction of the Tuoba Hydropower Station, it was archaeologically excavated by the Yunnan Provincial Institute of Cultural Relics and Archaeology from February to October 2022. An excavation area of 4000 m^2 uncovered more than 5000 artifacts, which included pottery, lithics, metal objects (copper or iron), and organic remains (bone or wood). Based on the cultural remains, the site has been dated to the Late Neolithic to the Iron Age.

The site is topographically partitioned into two distinct zones: Area I, a ring-shaped lowland encircling the terrace, and Area II, a circular elevated region located atop the terrace (Fig. 2a). Area I comprises stratified sedimentary deposits forming a gradual slope, characterized by a gradational sequence of layers—thinner and finer-grained deposits proximal to the terrace, transitioning to thicker, coarser-grained units distally. The maximum thickness of the deposits in this area reached up to approximately 3.8 m below the surface, with archaeological stratigraphy analysis identifying 14 distinct stratigraphic units. In contrast, Area II exhibits a radially outward-dipping stratigraphic sequence, sloping downward from its central axis toward the periphery. Sedimentological investigations reveal variable thicknesses within this zone, with maximum accumulation depths exceeding 4.6 m. The stratigraphy here comprises 17 stratified units, including 5 well-defined anthropogenic activity surfaces interspersed within the depositional sequence, indicative of repeated land-use episodes.

A total of 238 archaeological features were identified across both areas. Area I has fewer and less diverse features, which primarily comprise pits, ditches, residential structures, and stone walls. Notably, a prominent circular ditch was observed, potentially indicative of an encircling defensive or ritual trench. In contrast, Area II exhibits significantly greater complexity and functional diversity. This area includes 83 ash pits, 29 ash ditches, 32 residential structures (classified as stone-constructed, semi-subterranean, or stilted), 55 infant burials, and

11 furnaces clustered in the central zone. Additionally, 5 kilns were documented: 2 large semi-subterranean prehistoric kilns and 3 Ming-Qing dynasty pottery kilns. The spatial concentration of these features suggests specialized activity zones, particularly in metallurgy and ceramics production.

The archaeological settlement demonstrates a spatially segregated functional zonation pattern characterized by three distinct sectors: domestic habitation, animal husbandry, and metallurgical production. Human dwellings were systematically demarcated from livestock enclosures through constructed barriers of drystone masonry and timber palisades, while the central smelting complex was strategically encircled with protective perimeter fortifications (Fig. 2b). The terraced settlement’s defensive infrastructure comprised multiple concentric security layers: an inner wooden palisade demarcating the inhabited plateau, supplemented by an exterior defensive perimeter trench incorporating funnel-shaped access control points. Structural investigations reveal sophisticated building technologies employing load-bearing stone foundations supporting composite wall systems of timber framing and rammed earth construction. Architectural elements include dual columnar systems (interior structural columns and peripheral eave supports), precisely engineered pillar bedding grooves, central hearth installations with integrated drainage channels, and specialized lithic anchoring stones for structural stabilization. This construction methodology demonstrates advanced understanding of load distribution and environmental adaptation. The spatial organization reflects proto-urban planning principles, harmonizing functional separation with integrated defensive considerations.

Stratigraphic analysis of Area II (Fig. 2c), relying on soil texture, color, and unearthed artifacts, categorizes the site into four distinct phases. Phase I, located beneath Layer ⑨, is attributed to the Late Neolithic period. This phase serves as a crucial baseline for understanding the early human-environmental interactions in the region. Phase II, encompassing Layers ⑩–⑨, marks the transitional era from the Neolithic to the Bronze Age. This transition phase is a key period for tracing the technological and cultural shifts that occurred as human societies advanced from simple stone-tool-using communities to those with emerging metal-working capabilities. Phase III, represented by Layers ⑧–⑥, corresponds to the Mid-Late Bronze Age. Notably, Layer ④ stands out as the thickest cultural deposit within this phase, indicating a period of relatively intensive human occupation and activity. This thickness may suggest prolonged settlement, a large population, or significant cultural development during this time. Phase IV, represented by Layer ②, spans from the Late Bronze Age to the Iron Age. This phase captures the dynamic changes in human society as it adapted to new metallurgical technologies. Layer ①, on the other hand, is composed of modern sediments, providing a reference for understanding contemporary environmental processes at the site. The well-preserved cultural

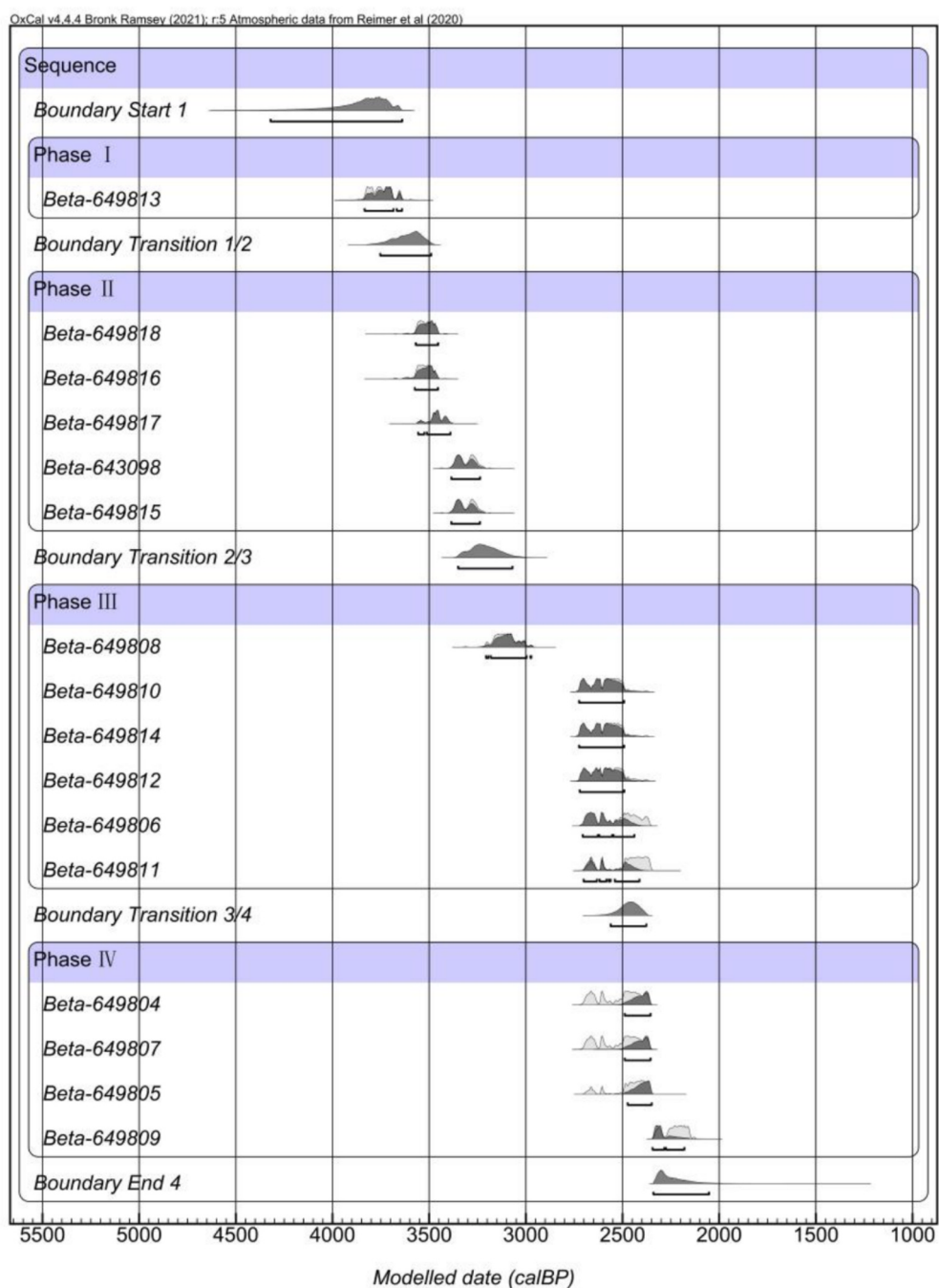


Fig. 3. Bayesian age model for Jicha ^{14}C dates.

deposits at this site offer invaluable perspectives on the utilization of plant resources in Northwest Yunnan. These deposits not only record the types of plants used by ancient communities but also provide clues about the changing patterns of plant exploitation over time, reflecting the evolving relationship between humans and their natural environment in this region.

2.2. Research methods

2.2.1. AMS radiocarbon dating

Sixteen samples, encompassing plant seeds, charcoal, and human bones from burial sites, were selected from distinct stratigraphic units for Accelerator Mass Spectrometry (AMS) radiocarbon dating (Table 1). The provenance of these samples is as follows: From Phase I, a single rice

sample was retrieved from an ash-filled ditch. From Phase II, 5 samples were collected from diverse units. This included 3 rice samples sourced from a burial, a stove, and an activity surface, respectively. Additionally, 2 human bone samples were obtained from a burial and a ditch. From Phase III, 6 samples were collected, comprising 4 human bone samples from burials, 1 wheat grain from a house, and 1 rice sample from a hearth. From Phase IV, 4 samples were collected: 1 rice sample from a house, 1 wheat sample from a kiln, and 2 human bone samples from burials. The AMS radiocarbon dating was carried out at the Beta Analytic Lab in Florida, USA. The obtained dating results were calibrated using the OxCal v4.4.4 software and the IntCal20 calibration curve (Reimer et al., 2020). This approach ensures the scientific rigor and accuracy of the dating process, providing reliable chronological data for further archaeological research.

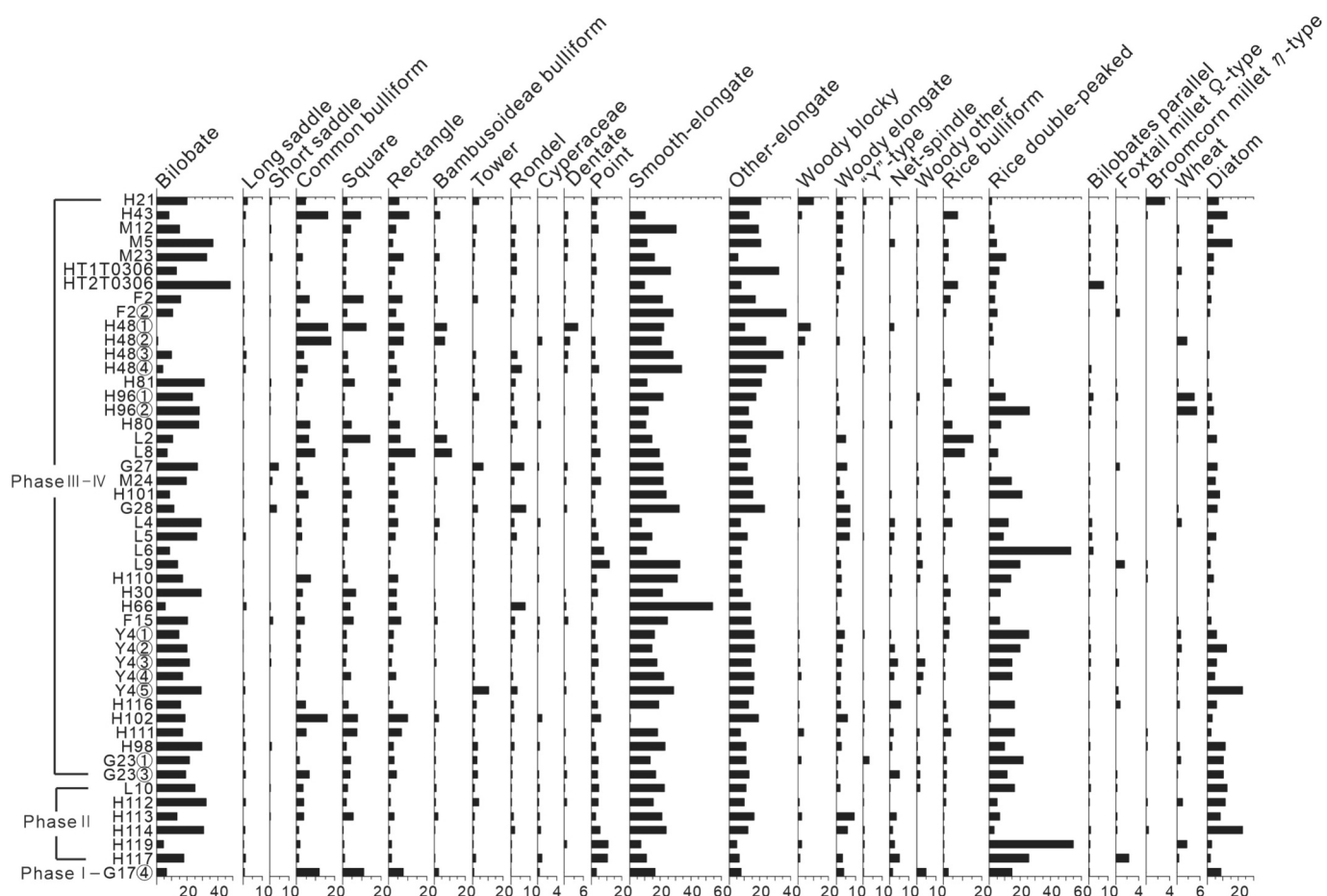


Fig. 4. Percentage diagram of major phytolith types at the Jicha site.

2.2.2. Phytolith extraction and analysis

Area II of the Jicha site, designated as a central zone of early human occupation, constitutes the primary focus of this study. A systematic sampling strategy was employed to select 49 representative archaeological features across stratigraphic units, guided by established phasing methodologies. For phytolith analysis, soil samples (100 g each) were retrieved from distinct depositional contexts across 4 defined phases. In Phase I, a single sample was collected from a ditch feature. Phase II involved 6 samples, comprising 5 specimens from ash pit contexts and 1 from a hearth. The most extensive sampling occurred during Phase III, where 35 samples were obtained from diverse contexts: 14 from ash pits, 5 from ditches, 5 from hearths, 5 from kiln sites, 3 from tombs, 2 from fire pits, and 1 from a house structure. Finally, Phase IV included 7 samples, with 4 derived from ash pits, 2 from domestic structures, and 1 from a tomb. All contextual data—stratigraphic phasing, sub-period categorization, excavation unit coordinates, and feature typology—are systematically cataloged in Table S1, ensuring replicability and facilitating comparative analysis.

Phytoliths were isolated from soil samples following the heavy liquid separation protocol established by Wang and Lu (1992). Soil specimens were initially dried at low temperature in a controlled oven to eliminate moisture interference. For each extraction, 3.0 ± 0.1 g of homogenized, fine-textured soil was subjected to sequential chemical treatments: initial oxidation with excess 30 % H_2O_2 , followed by acid digestion using 10 % HCl. A standardized *Lycopodium* spore tablet (27,560 spores/grains) was incorporated as a quantitative marker. Phytoliths were separated via density gradient centrifugation using zinc bromide ($ZnBr_2$) heavy liquid adjusted to a specific gravity of 2.35. The resulting phytolith concentrate was rinsed with anhydrous ethanol and mounted onto microscope slides using neutral gum. Slides were examined under a

Nikon E200 microscope at $400 \times$ magnification for phytolith identification and counting.

Counting focused on well-preserved phytolith morphotypes exhibiting distinct diagnostic characteristics. Phytoliths from Poaceae and woody plants were identified primarily following Wang and Lu (1992). Criteria for identifying crop phytoliths were adopted from Ge et al. (2022), Weisskopf and Lee (2016), Wen et al. (2018), and Ball et al. (2009, 2017). The classification employed established traditional nomenclature for phytolith morphotypes.

For statistical analysis, a target of over 300 phytoliths per sample was counted where feasible. For 4 samples with low phytolith concentrations (H21, H48①, H48②, H102), all recovered phytoliths were counted. Experimental data indicate differential phytolith production rates among rice, foxtail millet, and common millet husks; phytolith yields from foxtail and common millet husks generally reflect relative crop abundance, whereas rice husk phytolith production is comparatively lower (Zhang et al., 2010).

The relative abundance of each crop within the crop assemblage was calculated as the proportion of its diagnostic phytoliths relative to the total crop phytolith sum. Additionally, the contribution of rice to the overall phytolith assemblage was calculated as the percentage of diagnostic rice morphotypes (including rice bulliform, parallel bilobates, and double-peaked phytoliths) relative to the total number of phytoliths identified. Phytolith percentage diagrams, incorporating CONISS cluster analysis, were generated using Tilia (v. 2.6.1). Bubble charts and crop proportion graphs were created using Excel 2019, Adobe Illustrator (v. 26.0.0), and Origin 2022.

Modern studies on rice cultivation demonstrate that the ratio of sensitive (S) phytoliths (those influenced by plant water status, e.g., long and stomatal cells) to fixed (F) phytoliths (genetically determined forms,

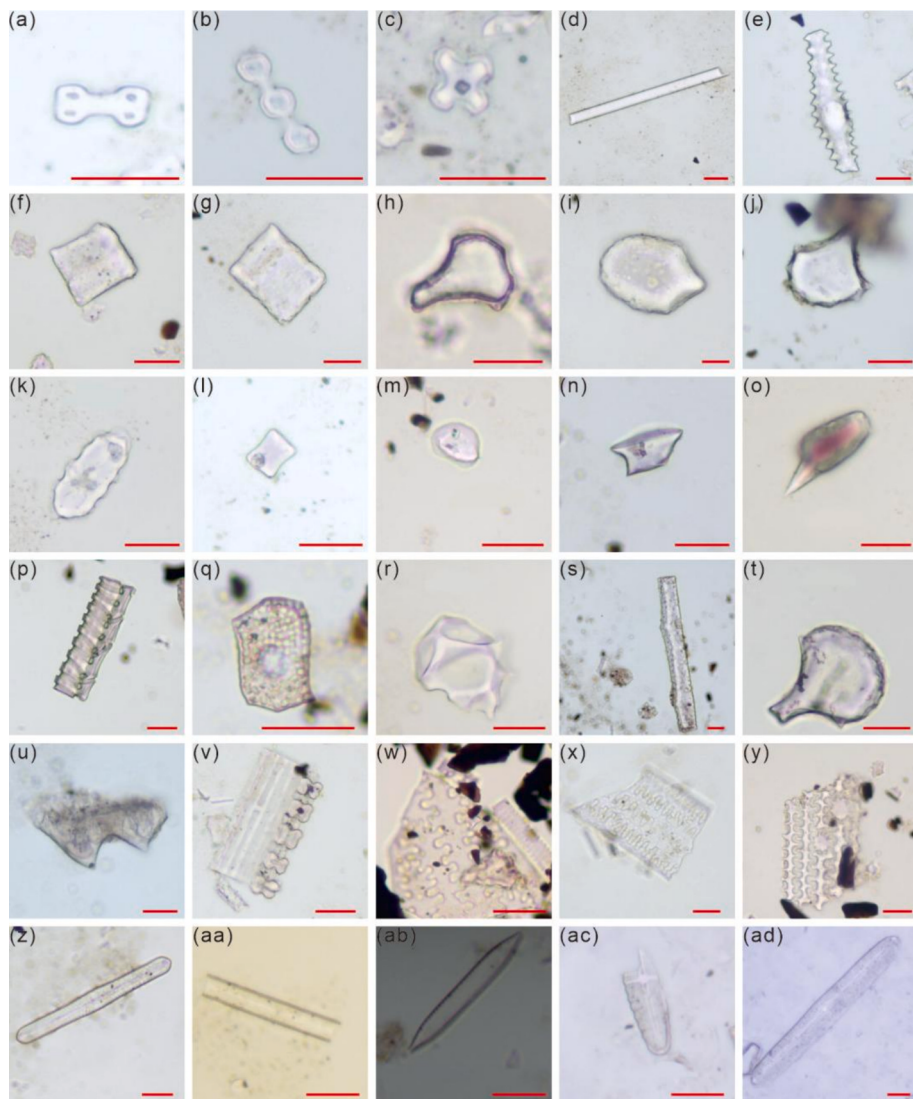


Fig. 5. Representative phytoliths and diatoms from the Jicha site: (a) Bilobate; (b) Polylobate; (c) Cross-shaped; (d) Smooth-elongate; (e) Echinate-elongate; (f) Square; (g) Rectangular; (h) Common bulliform; (i) Scutiform-bulliform from reed; (j) Bambusoideae bulliform; (k) Dentate; (l) Saddle(long); (m-n) Rondel; (o) Point; (p) Oblong tracheid; (q) Cyperaceae polygonal; (r) Woody blocky; (s) Woody elongate; (t) Rice bulliform; (u) Rice double-peaked; (v) Rice parallel bilobates; (w) Foxtail millet Ω-type; (x) Common millet η-type; (y) Inflorescence bract from wheat; (z) *Pinnularia*; (aa) *Fragilaria ulna*; (ab) *Nitzschia palea*; (ac) *Achnanthes brevipes*; (ad) *Pinnularia major*; Scale bar = 20 μ m.

e.g., short cells such as bilobate, saddle, and rondel) can serve as an effective proxy for reconstructing paddy field moisture levels (Jenkins et al., 2016; Weisskopf et al., 2015b; Weisskopf, 2017). In this study, we applied this S/F phytolith morphological model to samples containing abundant rice phytoliths (>6900 grains/g) to assess the moisture conditions of the ancient rice farming system at the Jicha site.

3. Results

3.1. AMS radiocarbon dating results

Sixteen AMS ^{14}C dates were obtained from the Jicha site, yielding calibrated ages spanning from 3800 to 2200 cal BP (Table 1; Fig. 3; Fu et al., 2024). These chronological data demonstrate strong coherence with the site's established archaeological phases.

Phase I is characterized by a single date obtained from a rice seed recovered in gully 2022WJG17④, yielding a calibrated age range of 3837–3687 cal BP. Phase II is defined by dated materials (rice and human bone) that cluster within the calibrated age range of ca. 3600–3300 cal BP. Phase III exhibits calibrated ages for wheat and

human bone spanning ca. 2800 to 2300 cal BP. A charcoal sample (2022WJL2) from this phase yielded a calibrated age of 3209–3000 cal BP, a date that significantly conflicts with all other results from Phase III. Due to the potential “old wood effect” inherent in charcoal, this date was excluded in favor of results from short-lived materials (seeds and bone), which more reliably anchor the timing of human activity. Phase IV includes dated materials (wheat, rice, and human bone) with calibrated age ranges spanning ca. 2800–2200 cal BP (Fig. 3). Notably, the calibrated age distributions of Phases III and IV demonstrate significant chronological overlap, complicating precise temporal separation. Consequently, the datasets from these two phases are analyzed collectively in subsequent discussions.

Based on systematic radiometric analyses and stratified archaeological evidence, Area II at the Jicha site demonstrates an extended occupation sequence spanning multiple cultural phases. The archaeological chronology of the site demonstrates continuous human occupation spanning from the Late Neolithic period through the Iron Age, with the principal phase of occupation dated to the Middle to Late Bronze Age. The established temporal framework is divided into the following periods characterized by radiocarbon dating:

Phase I (Late Neolithic): calibrated radiocarbon dates indicate occupation from 3800 to 3600 cal BP, marking the site's earliest settlement phase.

Phase II (Neolithic-Bronze Age Transition): The subsequent phase (3600–3300 cal BP) reflects a cultural transition marked by technological innovations, including the gradual adoption of metallurgical practices alongside residual Neolithic traditions.

Phases III-IV (Middle-Late Bronze Age to Iron Age): This later phase represents the site's most intensive occupation and is characterized by advanced bronze metallurgy, fortified architectural features.

3.2. Phytolith results

The 49 archaeological samples recovered from Area II of the Jicha site revealed a highly diversified assemblage of phytoliths, with a total of 24,072 individual specimens classified into 35 distinct morphological categories (Fig. 4). This phytolith assemblage exhibited a tripartite taxonomic distribution, encompassing crop-derived phytoliths, Poaceae grass phytoliths, and woody plant phytoliths. Crop-associated phytoliths demonstrated clear taxonomic specificity, including: rice (*Oryza sativa*): characterized by scalloped bulliform, double-peaked, and parallel bilobate morphotypes; foxtail millet (*Setaria italica*): identified through Ω-type phytoliths; common millet (*Panicum miliaceum*): represented by η-type phytoliths; and wheat (*Triticum* spp.): evidenced by silicified epidermal tissues. The Poaceae grass phytolith assemblage displayed significant morphological diversity, including bilobate, polylobate, cross-shaped, long/short saddle-shaped, square/rectangular blocky, common bulliform, dentate, trapeziform, point, rondel, Cyperaceae polygonal, smooth-elongate, other elongate types, tracheary elements, and additional undetermined forms. Woody plant phytoliths exhibited characteristic morphologies such as woody blocky, woody elongate, woody tabular, net-spindle, globular granulate, woody Y-type, and other undifferentiated forms (Fig. 5). The comprehensive phytolith record provides critical evidence for reconstructing the paleoecological context and subsistence strategies of the site's occupants during the investigated period.

Phytolith analysis from the Jicha site offers critical insights into the subsistence strategies and environmental adaptations during its occupation (Fig. 4). Crop-derived phytoliths accounted for 15.71 % of the total assemblage, predominantly composed of rice bulliform and rice husk morphotypes. Rice phytoliths demonstrated universal presence (100 % site-wide occurrence) and comprised 94.55 % of all crop phytoliths. Secondary crops included foxtail millet (detected in 44.90 % of samples; 1.41 % of crop phytoliths), common millet (detected in 16.33 % of samples; 0.30 % of crop phytoliths), and wheat (detected in 53.06 % of samples; 3.74 % of crop phytoliths). Non-crop Poaceae phytoliths dominated the overall assemblage (78.17 %), characterized by bilobate and smooth-elongate morphotypes that likely originated from wild grasses or post-harvest crop residues. Woody plant phytoliths contributed 6.12 % of the total, primarily elongate forms and other arboreal types, suggesting limited tree cover or controlled woody resource utilization.

Accompanying micropaleontological analysis recovered 1463 diatom frustules from stratified contexts, with taxonomic identification revealing *Nitzschia palea* as the dominant species. Other identified taxa included *Achnanthes brevipes* var. *intermedia*, *Pinnularia major*, *Pinnularia stomatophora*, and *Fragilaria ulna* (Fig. 5). Qualitative diatom analysis suggests these assemblages potentially reflect localized hydrological dynamics and thermal regimes, with implications for reconstructing ancient microenvironments (Wang et al., 2018, 2022; Zhang et al., 2023). These findings collectively suggest a rice-dominated agro-ecosystem integrated with secondary crops, supported by evidence of controlled water management practices, as inferred from both phytolith and diatom records.

Analyzing phytolith assemblages across diverse chronological periods provides valuable perspectives on the ancient human utilization of

plant resources. At the Jicha site, based on archaeological stratigraphy and chronological data derived from 49 archaeological samples, we delineated phytolith assemblage zones by categorizing the phytolith data according to chronologically defined phases, thus uncovering patterns in ancient plant resource utilization.

Phase I yielded 533 phytoliths in the single sample. Rice phytoliths made up 17.45 % of the entire phytolith assemblage in Phase I. Among crop-related phytoliths, double-peaked phytoliths were the most abundant, accounting for 17 % of the total assemblage. Rice bulliform and parallel bilobate phytoliths were also detected. Non-crop Poaceae phytoliths constituted 71.67 % of the total phytolith assemblage. Elongate phytoliths were the most commonly occurring type, representing 24.39 %. Other notable phytolith types included bilobate (17 %), common bulliform (12 %), and blocky (10 %) phytoliths. Woody phytoliths accounted for 10.88 %, with woody elongate phytoliths being the predominant form, making up 8 %. Furthermore, 46 diatom frustules were recovered, all of which were identified as *Nitzschia palea*. This finding implies the presence of favorable hydrothermal conditions at the site during the relevant period.

Phase II involved the examination of 6 samples, from which a total of 3394 phytoliths were successfully identified. Crop phytoliths, including rice, foxtail millet, common millet, and wheat, constituted 22.51 % of the overall phytolith assemblage. Among these, rice phytoliths were the most prevalent, accounting for 93.98 % of all crop phytoliths, and were ubiquitous (100 % occurrence). In contrast, foxtail millet, common millet, and wheat phytoliths made up 1.96 %, 0.39 %, and 3.66 % of the crop phytoliths respectively, with occurrence frequencies of 83.3 %, 50 %, and 66.6 %. Non-crop Poaceae phytoliths were the dominant group in the total phytolith assemblage, representing 69.71 %. They were primarily composed of bilobate and elongate types. Woody phytoliths accounted for 7.78 % of the assemblage, with woody blocky, woody elongate, and net-spindle types being the predominant forms. Moreover, 329 diatom frustules were recovered. The identified diatom taxa included *Nitzschia palea*, *Achnanthes brevipes* var. *intermedia*, *Pinnularia major*, *Pinnularia stomatophora*, and *Fragilaria ulna*. The presence of these diatoms strongly indicates the existence of favorable hydrothermal conditions at the site.

Phases III and IV incorporated 42 samples, resulting in the identification of a total of 20,145 phytoliths. Crop phytoliths accounted for 15.41 % of the total phytolith assemblage and included the same crop types as in Phase II: rice, foxtail millet, common millet, and wheat. Rice phytoliths remained the dominant crop phytolith type, accounting for 94.52 % of all crop phytoliths and were present in 100 % of the samples. Foxtail millet, common millet, and wheat phytoliths constituted 1.32 %, 0.29 %, and 3.87 % of the crop phytoliths respectively, with occurrence frequencies of 42.86 %, 14.29 %, and 54.76 %. Non-crop Poaceae phytoliths were the most abundant in the total phytolith assemblage, representing 78.53 %. They mainly consisted of bilobate and elongate types, along with some less frequently occurring forms. Woody phytoliths accounted for 6.06 % of the assemblage, with the same predominant types (woody blocky, woody elongate, and net-spindle) as in Phase II. Additionally, 1,088 diatom frustules were identified, and the species were consistent with those found in Phase II, further suggesting the persistence of favorable hydrothermal conditions at the site.

3.3. Ratio of sensitive to fixed phytoliths

The Jicha site yielded a diverse assemblage of rice phytolith morphotypes, including bulliform, double-peaked, and parallel bilobate forms. This morphological diversity not only confirms localized rice cultivation practices but also enables detailed ecological assessments of the associated agricultural system. Adherence to the diagnostic criteria established by Weisskopf et al. (2015b) demonstrated that the majority of sampled phytolith concentrations met or exceeded the threshold required for reliable S/F ratio analysis. Chronological analysis of the assemblages revealed significant temporal variations in phytolith

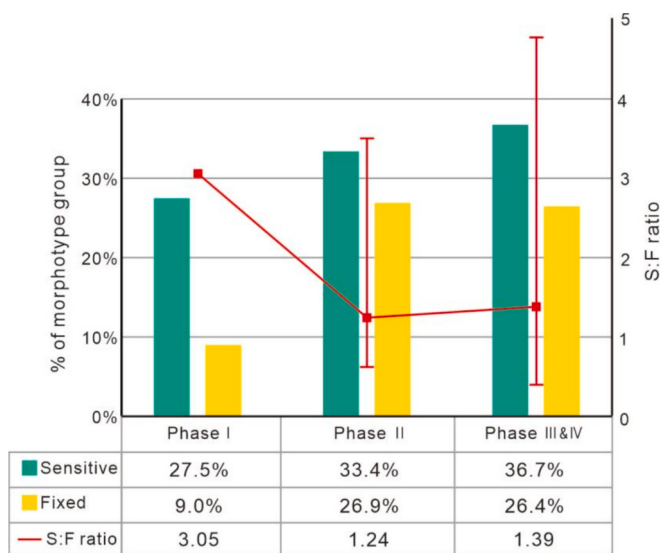


Fig. 6. Percentage of sensitive versus fixed phytolith morphotypes in the three phases; S/F > 1 indicates wetland rice cultivation, while S/F < 1 suggests upland rice cultivation; red error bars represent the S/F ratio ranges in various archaeological contexts; percentages exclude all phytolith types not within the sensitive/fixed classification defined by Weisskopf et al. (2015b).

composition across three distinct phases: the mean percentages of sensitive phytoliths during Phases I, II, and III-IV were 27.5 %, 33.4 %, and 36.7 %, respectively, while fixed phytoliths constituted 9 %, 26.9 %, and 26.4 %. These compositional shifts translated to S/F ratios of 3.05 (Phase I), 1.24 (Phase II), and 1.39 (Phase III-IV), respectively (Fig. 6). The observed pattern suggests evolving agricultural intensification through time, with Phase I exhibiting the highest relative abundance of sensitive phytoliths—a characteristic often associated with less intensive cultivation practices. Subsequent phases show increased proportions of fixed phytoliths, potentially reflecting enhanced soil disturbance and more intensified rice farming strategies.

4. Discussion

4.1. Agricultural structure of the Jicha site and northwestern Yunnan settlements

The phytolith assemblage from the Jicha site offers insights into a dynamic agricultural evolution, characterized by the co-existence of cultivated and wild plant resources across three cultural phases:

Phase I: Late Neolithic Period (ca. 3800–3600 cal BP). Archaeological remains from this period are scarce. Nevertheless, a small number of rice remains, one dated to 3837–3687 cal BP via AMS ^{14}C dating, along with a relatively large quantity of rice phytoliths, were discovered. These findings strongly suggest that agriculture had emerged by this time, with rice farming as the predominant agricultural practice.

Phase II: Neolithic-Bronze Transitional Period (ca. 3600–3300 cal BP). Rice continued to be the dominant crop. However, around 3500 cal BP, rainfed crops such as wheat, foxtail millet, and common millet began to appear. Among these, wheat was the most abundant, followed by a slightly higher proportion of foxtail millet than common millet. This shift indicates a transition towards a mixed farming system, where rice remained the primary crop but was supplemented by dryland crops.

Phase III-IV: Middle-Late Bronze Age to Iron Age (ca. 2800–2200 cal BP). Rice farming maintained its dominance. Although the overall quantity of dryland crops did not increase significantly compared to Phase II, the proportion of wheat among them did rise. This implies that the agricultural system remained primarily rice-based, with dryland crops serving as a supplementary component.

In summary, the co-existence of rice, foxtail millet, common millet, and wheat at the Jicha site reflects a diversified agricultural system. The introduction of dryland crops in Phase II did not undermine the primary importance of rice cultivation. Instead, the agricultural strategy evolved from a predominantly rice-based system to a mixed farming system, with dryland crops complementing rice, while rice cultivation remained crucial.

Systematic archaeobotanical analyses in northwestern Yunnan have primarily focused on the Baiyangcun and Haimenkou sites. The Baiyangcun site, dating back to the Late Neolithic period (ca. 4700–3600 cal BP), reveals a rice-dominated agricultural economy, with millet as a supplementary crop (Dal Martello et al., 2018; Dal Martello, 2020). The Haimenkou site, spanning the Late Neolithic to Bronze Age (ca. 3600–2500 cal BP), shows shifting crop patterns, generally dominated by millet, followed by rice, and a notable increase in wheat after ca. 3400 cal BP (Dal Martello, 2020; Xue et al., 2022). Further south in western Yunnan, sites like Xinguang (ca. 4450–4000 cal BP) and Yingpanshan (ca. 3800 cal BP) have only yielded rice remains (Dal Martello, 2020; Yao, 2010; Zhao and Chen, 2011). At the Shilinggang site, analysis of charred seeds and phytoliths indicates the presence of both rice and millet, with rice being the dominant crop (Li et al., 2016; Zhang et al., 2017).

The archaeobotanical record shows distinct temporal and spatial variations in agricultural practices across western Yunnan from the Late Neolithic to the Bronze Age. This heterogeneity is likely due to the region's diverse topography and climatic conditions, which necessitated localized adaptive strategies for optimizing agricultural yields. Additionally, the influence of human migrations and cultural exchange on shaping these agricultural practices cannot be overlooked, as they may have introduced new crops and farming techniques.

The charred rice discovered at the Jicha site (ca. 3800 cal BP) provides the earliest direct evidence of rice cultivation within the Three Parallel Rivers region, a crucial corridor of the Tibetan-Yi Corridor. Notably, the absence of contemporaneous millet remains, a crop typically associated with diffusion from the northern Yellow River Basin, complicates interpretations of the transmission routes of rice into the region. Earlier evidence of charred rice in surrounding regions, such as the Baodun site to the north (ca. 4600 cal BP; Guedes et al., 2015), the Guijiaobao site to the east (ca. 5000 cal BP; Huan et al., 2022), and the Baiyangcun site to the southeast (ca. 4700 cal BP; Dal Martello, 2020), suggests multiple potential source areas. The Xinguang site, located to the south, might also contain earlier evidence of rice, although direct radiocarbon dating of rice grains is currently unavailable. Given these uncertainties, the mechanisms of agricultural dispersal to Jicha remain speculative and require further investigation.

4.2. Phytolithic insights into wild plant resource utilization

Phytolith analysis at the Jicha site indicates a primary reliance on rice agriculture since the Late Neolithic period. However, a significant proportion of non-crop phytoliths, especially those derived from woody plants, persisted throughout all cultural phases. Due to morphological constraints, current methodologies for classifying woody phytoliths from the floristically diverse southwestern region are limited, hindering precise taxonomic identification (Wang et al., 2022). At Jicha, most woody phytoliths are generically classified as either “woody elongate” or “other woody” types, precluding precise taxonomic identification. Consequently, analysis can only tentatively associate some phytoliths with broad-leaved angiosperms, while blocky morphotypes may potentially derive from gymnospermous species (Wang and Lu, 1992).

Furthermore, various herbaceous phytoliths, referred to as the other non-crop phytolith types, were present throughout all phases. Among these, rondel and dentate phytoliths likely originated from C₃ plants (Ge, 2016), while the consistent occurrence of collapsed saddle and bambusoid bulliform phytoliths suggests the continuous growth of bamboo near the site, indicating possible sustained human utilization of bamboo

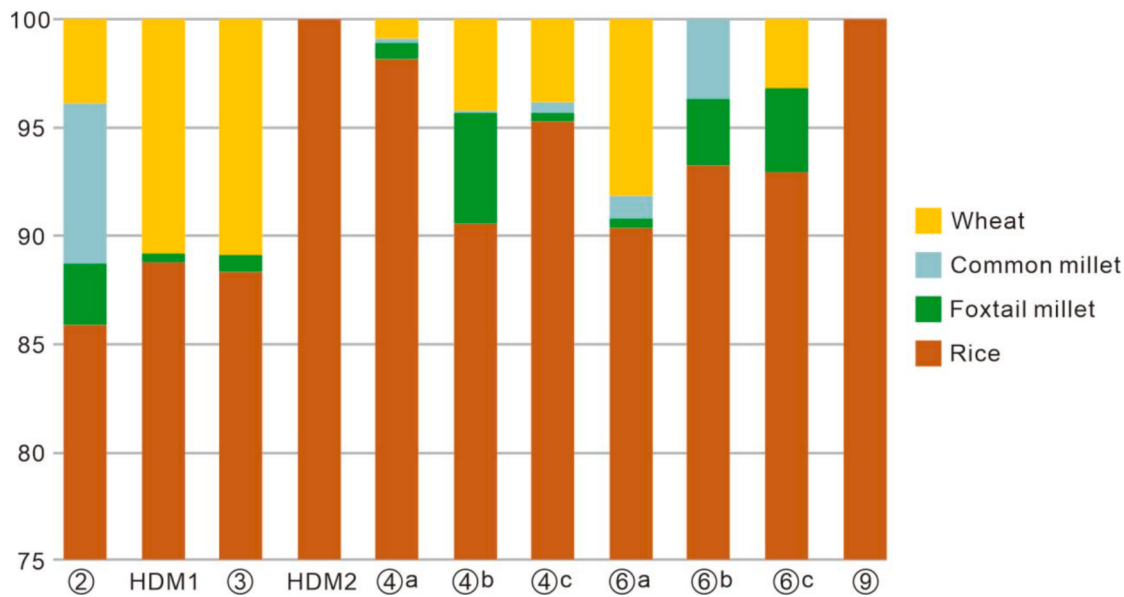


Fig. 7. Accumulation histogram of crop phytoliths in the strata of Area II, Jicha site.

resources. However, certain phytolith types (e.g., bilobate, rectangular, common bulliform, and elongate) were excluded from detailed discussion due to indeterminate botanical origins.

Previous flotation analyses at the site have yielded a variety of macrobotanical remains, including seeds of staple crops, fruit shells, and various other wild plant remains. This suggests that the inhabitants of Jicha supplemented their agricultural diet by foraging for wild fruits from the surrounding environment, a practice readily explainable given Yunnan's diverse and abundant flora.

In summary, the evidence suggests that the Jicha community adopted a comprehensive and efficient strategy of utilizing local wild plant resources to complement their agricultural practices.

4.3. Agricultural cultivation and management practices of the Jicha inhabitants

The archaeobotanical record from the Jicha site indicates that rice cultivation emerged around 3800 cal BP, followed by the appearance of dryland crops (foxtail millet, common millet, and wheat) after ca. 3500 cal BP. Throughout the site's occupation, rice farming consistently dominated the agricultural structure, with dryland agriculture serving as a supplement. It is well-known that rice agriculture is better adapted

to warm and humid climatic conditions, whereas dryland crops such as millet can thrive even under relatively arid conditions. Paleoclimatological studies in Southwest China indicate that during the Late Holocene (since ca. 4000 BP), the overall climatic trend in this region became cooler, drier, and characterized by frequent fluctuations (Wang et al., 2020, 2023; Xiao et al., 2018; Zhang et al., 2016, 2020). This reveals a certain incongruity between the site's dominant agricultural characteristics and the prevailing climatic background, suggesting that the agricultural model at Jicha was not solely reliant on rain-fed farming.

Significant evidence comes from the analysis of the ratio between sensitive and fixed phytoliths. The results show that in all three phases, sensitive phytoliths were consistently more abundant than fixed types, with S/F ratios of 3.05, 1.24, and 1.39, respectively. This indicates that rice cultivation at Jicha consistently benefited from ample water resources, implying that the inhabitants may have employed certain irrigation techniques. Furthermore, the consistent presence of diatoms, which are sensitive to aquatic environments, in relatively high proportions within the samples also points to favorable water conditions in the agricultural fields surrounding the site. Finally, the low abundance of weed phytoliths (e.g., from Cyperaceae) across the samples suggests a minimal presence of weeds in the rice paddies. This indicates that the Jicha inhabitants likely practiced deliberate field management and

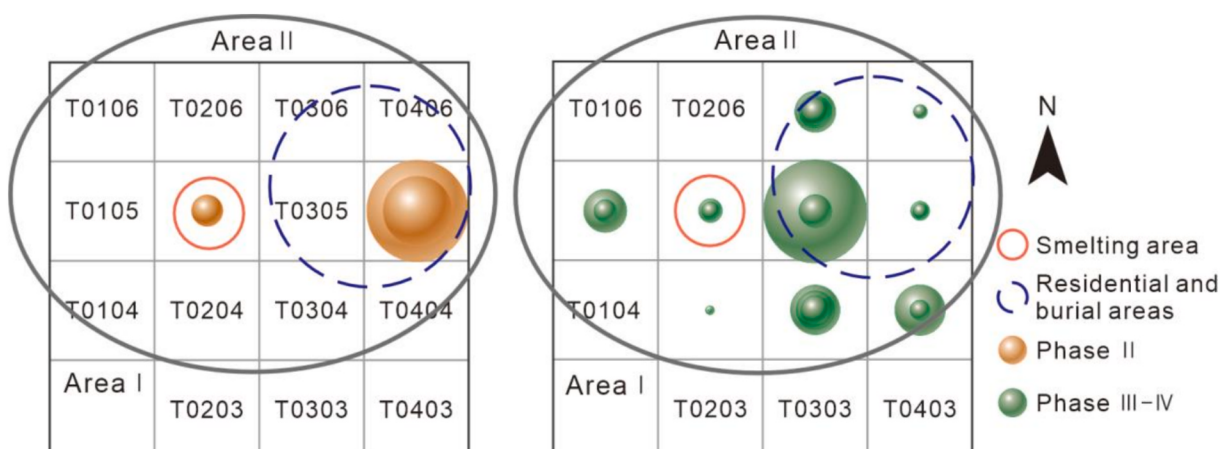


Fig. 8. Bubble chart of the spatial and temporal distribution of rice husk content in Jicha site (bubble size = phytolith concentration (particles/g)).

weed control to optimize cultivation conditions. Overall, the cultivation techniques and field management strategies adopted by the Jicha people likely played a crucial role in their agricultural success and resilience.

A comparison of trends in the percentage abundance of phytoliths from dryland crops and rice across 11 consecutive archaeological stratigraphic units reveals a significant negative correlation between the cultivation proportions of wheat and rice (Fig. 7). This finding is confirmed through Pearson correlation analysis ($r = -0.769, p < 0.05$). This suggests that the inhabitants of the Jicha site optimized field management and improved production efficiency by intentionally adjusting the quantities of various crops to adapt to environmental changes. Such adjustments allowed them opportunities to engage in other subsistence activities, thereby ensuring the diversification of their survival strategies.

4.4. Crop processing and management systems of the Jicha inhabitants

From harvest to consumption, crops go through several stages, including threshing, winnowing, storage, and processing. Different stages of crop processing yield distinct byproducts. Analysis of phytolith assemblages can reveal crop processing patterns and locations, thereby facilitating discussions on functional zoning within archaeological sites (Harvey and Fuller, 2005). Threshing and winnowing separate straw, leaves, weed seeds, and immature grains, all of which may become incorporated into byproducts. In later processing stages such as dehusking, substantial quantities of glume phytoliths are typically deposited. Previous studies suggest that the widespread spatial distribution of dehusking residues (e.g., concentrated husk phytoliths) indicates large-scale, collective crop processing activities at a site (Weisskopf et al., 2015a).

Phytoliths from rice exhibit distinct morphological types corresponding to different plant parts, enabling the reconstruction of ancient harvesting and processing practices through phytolith assemblage analysis. In Area II of the Jicha site, agricultural phytoliths were predominantly derived from rice glumes, with minor contributions from stems and leaves. Based on radiocarbon dating and phytolith assemblage data, the temporal and spatial variations in crop distribution at the site are analyzed and presented in three major distinct stages, illustrated through bubble plots (Fig. 8).

In Phase I, the paucity of archaeological features precluded a comparative spatial analysis of crop processing. However, the notable presence of rice double-peaked phytoliths suggests that dehusking was already a well-established agricultural practice among the site's inhabitants.

In Phase II, contexts H117, H119, and L10 showed high concentrations of rice husk phytoliths, mainly in excavation unit T0405. This indicates that by this time, the Jicha inhabitants conducted large-scale crop processing across an extensive site, with these activities focused in the eastern section of Area II, as supported by previous studies (Weisskopf et al., 2015a).

In Phase III-IV, features rich in rice husk phytoliths were distributed around a central platform area. The processing zone expanded compared to Phase II, potentially indicating further intensification of rice agriculture. This large-scale agricultural production likely provided a crucial economic and material basis for the site's sustained development.

The substantial presence of husks may also be linked to the storage practices of the early inhabitants. During fieldwork, flotation analysis of samples from kiln site 2022WJY4 recovered abundant seed remains, predominantly in the form of dehusked or unhusked grains. This finding suggests that the prevalence of rice husks could be associated with the grain storage strategies of the Jicha people, with such storage facilities often located within residential areas.

Based on the aforementioned analysis, it can be inferred that the inhabitants were engaged in large-scale grain harvesting and processing within specific zones, indicating a sophisticated capacity for social labor

organization. Furthermore, the crop processing area (or possibly storage zone) in eastern Area II during Phase II appears to have shifted to the vicinity of the central platform's metallurgical district during Phases III-IV. This transformation highlights a significant evolution in both the scale and spatial distribution of crop processing activities.

5. Conclusion

The Jicha site, dating to 3800–2200 cal BP, fills a critical gap in the prehistoric cultural sequence of northwestern Yunnan. Phytolith analysis of 49 samples from key archaeological features reveals an agricultural structure during the Late Neolithic to Bronze Age, characterized by a dominant rice-based system with the supplementary cultivation of wheat and minor millets, forming a mixed rice-dry farming economy.

Rice agriculture was already established in the region by 3800 cal BP. Between 3500 and 3300 cal BP, dry crops such as millet and wheat were introduced through cultural exchange, while rice remained the dominant crop. A significant negative correlation between wheat and rice percentages across stratigraphic layers suggests that the Jicha inhabitants adjusted crop ratios to adapt to environmental changes and optimize field management, thereby diversifying subsistence strategies and freeing labor for other activities. Beyond cultivated crops, abundant forest resources provided edible plants, including fruits and nuts, indicating broad-spectrum exploitation of local flora. The presence of dedicated crop-processing areas further demonstrates advanced labor organization and large-scale social production at the site.

CRediT authorship contribution statement

Xiabo Li: Writing – review & editing, Visualization, Software, Methodology, Investigation, Formal analysis, Data curation, Conceptualization. **Wuqi Zhang:** Writing – original draft, Visualization, Software, Methodology, Investigation, Formal analysis, Data curation, Conceptualization. **Qing Yang:** Writing – review & editing, Visualization, Validation, Supervision, Project administration, Methodology, Investigation, Funding acquisition, Conceptualization. **Changcheng Hu:** Investigation. **Nan Cheng:** Investigation. **Jie Fu:** Investigation. **Zining Zou:** Methodology, Investigation. **Yuanyuan Gao:** Investigation. **Hongbo Zheng:** Funding acquisition.

Declaration of competing interest

The authors declare that they have no known competing financial interests or personal relationships that could have appeared to influence the work reported in this paper.

Acknowledgements

This study was supported by the National Natural Science Foundation of China (NSFC) (42471181, 42361144879), The National Key R&D Program of China (2022YFF0801102), Yunnan Fundamental Research Projects (202301BF070001-005), Yunnan Revitalization Talent Support Program (for Q. Y.), Queensland-Chinese Academy of Sciences Collaborative Science Fund (QCAS036, 045GJHZ2023001MI).

Appendix A. Supplementary material

Supplementary data to this article can be found online at <https://doi.org/10.1016/j.jasrep.2025.105410>.

Data availability

Data will be made available on request.

References

- Ball, T.B., Ehlers, R., Standing, M.D., 2009. Review of typologic and morphometric analysis of phytoliths produced by wheat and barley. *Breed. Sci.* 59 (5), 505–512. <https://doi.org/10.1270/jbsbs.59.505>.
- Ball, T.B., Vrydaghs, L., Mercer, T., et al., 2017. A morphometric study of variance in articulated dendritic phytolith wave lobes within selected species of Triticeae and Aveneae. *Veg. Hist. Archaeobotany* 26, 85–97. <https://doi.org/10.1007/s00334-015-0551-x>.
- Dal Martello, R., 2020. Agricultural trajectories in Yunnan, Southwest China: a comparative analysis of archaeobotanical remains from the Neolithic to the Bronze Age. University of London, University College, London (United Kingdom).
- Dal Martello, R., 2022. The origins of multi-cropping agriculture in Southwestern China: archaeobotanical insights from third to first millennium BC Yunnan. *Asian Archaeol.* 6 (1), 65–85. <https://doi.org/10.1007/s41826-022-00052-2>.
- Dal Martello, R., Li, X.R., Fuller, D.Q., 2021. Two-season agriculture and irrigated rice during the Dian: radiocarbon dates and archaeobotanical remains from Dayingzhuang, Yunnan, Southwest China. *Archaeol. Anthropol. Sci.* 13 (4), 62. <https://doi.org/10.1007/s12520-020-01268-y>.
- Dal Martello, R., Min, R., Stevens, C., et al., 2018. Early agriculture at the crossroads of China and Southeast Asia: archaeobotanical evidence and radiocarbon dates from Baiyangcun, Yunnan. *J. Archaeol. Sci.-Reports* 20, 711–721. <https://doi.org/10.1016/j.jasrep.2018.06.005>.
- Fu, J., Li, Y., Hu, C., et al., 2024. Southbound transmission of metallurgy: new excavations at Jicha in the Hengduan Mountains, Yunnan. *Antiquity* 98 (400), e19.
- Ge, Y., 2016. Study on the Morphology and Application of Common Modern Plant Phytoliths in China. Ph.D. dissertation. University of Chinese Academy of Sciences, China.
- Ge, Y., Lu, H.Y., Wang, C., et al., 2022. Phytoliths in spikelets of selected Oryzoideae species: new findings from in situ observation. *Archaeol. Anthropol. Sci.* 14 (4), 73. <https://doi.org/10.1007/s12520-022-01544-z>.
- Guedes, J.A., Jiang, M., He, K.Y., et al., 2015. Site of Baodun yields earliest evidence for the spread of rice and foxtail millet agriculture to south-west China. *Antiquity* 87 (337), 758–771. <https://doi.org/10.1017/S0003598X00049449>.
- Harvey, E.L., Fuller, D.Q., 2005. Investigating crop processing using phytolith analysis: the example of rice and millets. *J. Archaeol. Sci.* 32 (5), 739–752. <https://doi.org/10.1016/j.jas.2004.12.010>.
- Huan, X.J., Deng, Z.H., Zhou, Z.Q., et al., 2022. The emergence of rice and millet farming in the Zang-Yi corridor of Southwest China dates back to 5000 years ago. *Front. Earth Sci.* 10, 874649. <https://doi.org/10.3389/feart.2022.874649>.
- Huo, R.L., Ren, L., 2022. Reconstruction and study of the transport network of the Southern Silk Road within China, based on GIS. *Geogr. Res.* 41 (04), 1122–1135.
- Jenkins, E., Jamjoum, K., Nuimat, S., et al., 2016. Identifying ancient water availability through phytolith analysis: an experimental approach. *J. Archaeol. Sci.* 73, 82–93. <https://doi.org/10.1016/j.jas.2016.07.006>.
- Li, P.R., 2020. Ethnic group research on "Zang-Yi Corridor" during the past 40 years. *J. Qinghai Nationalities University* 46 (03), 14–16.
- Li, H.M., Zuo, X.X., Kang, L.H., et al., 2016. Prehistoric agriculture development in the Yunnan-Guizhou Plateau, southwest China: Archaeobotanical evidence. *Sci. China Earth Sci.* 59, 1562–1573. <https://doi.org/10.1007/s11430-016-5292-x>.
- Lu, H.Y., Zhang, J.P., Wu, N.Q., et al., 2009a. Phytoliths analysis for the discrimination of foxtail millet (*Setaria italica*) and common millet (*Panicum miliaceum*). *PLoS One* 4 (2), e4448.
- Lu, H.Y., Zhang, J.P., Liu, K.B., et al., 2009b. Earliest domestication of common millet (*Panicum miliaceum*) in East Asia extended to 10,000 years ago. *PNAS* 106 (18), 7367–7372. <https://doi.org/10.1073/pnas.0900158106>.
- Reimer, P.J., Austin, W.E.N., Bard, E., et al., 2020. The IntCal20 Northern Hemisphere radiocarbon age calibration curve (0–55 cal kBP). *Radiocarbon* 62 (4), 725–757. <https://doi.org/10.1017/RDC.2020.41>.
- Shi, S., 2009. The Tibetan-Yi Corridor: Origins of Civilization and Ethnicity. Sichuan People's Publishing House, Chengdu.
- Wang, M., 2022. Research on Human Plant Resource Utilization and Environmental Adaptability of Xiaodong Site and Heping Culture. Ph.D. dissertation. Yunnan University, China.
- Wang, T.T., Wei, D., Jiang, Z.L., et al., 2022. Microfossil analysis of dental calculus and isotopic measurements reveal the complexity of human-plant dietary relationships in late Bronze Age Yunnan. *Archaeol. Anthropol. Sci.* 14 (5), 94. <https://doi.org/10.1007/s12520-022-01557-8>.
- Wang, Y.B., Shen, J., Wang, Y., et al., 2020. Abrupt mid-Holocene decline in the Indian Summer Monsoon caused by tropical Indian Ocean cooling. *Clim. Dyn.* 55, 1961–1977. <https://doi.org/10.1007/s00382-020-05363-7>.
- Wang, Y.J., Lu, H.Y., 1992. Research and Application of Plant Opal Phytoliths. Ocean Press, Beijing.
- Wang, X.X., Huang, X.Y., Sachse, D., 2023. Two-phase hydrological changes during the mid-to late Holocene transition in Southwest China. *Quat. Sci. Rev.* 322, 108432. <https://doi.org/10.1016/j.quascirev.2023.108432>.
- Wang, L., Jiang, W.Y., Jiang, D.B., et al., 2018. Prolonged heavy snowfall during the Younger Dryas. *J. Geophys. Res. Atmos.* 123 (24), 13748–13762. <https://doi.org/10.1029/2018JD029271>.
- Weisskopf, A., Deng, Z.H., Qin, L., et al., 2015a. The interplay of millets and rice in Neolithic central China: Integrating phytoliths into the archaeobotany of Baligang. *Archaeol. Res. Asia* 4, 36–45. <https://doi.org/10.1016/jара.2015a.1002>.
- Weisskopf, A., Qin, L., Ding, J.L., et al., 2015b. Phytoliths and rice: from wet to dry and back again in the Neolithic lower Yangtze. *Antiquity* 89 (347), 1051–1063. <https://doi.org/10.15184/агу.2015.94>.
- Weisskopf, A.R., Lee, G.A., 2016. Phytolith identification criteria for foxtail and broomcorn millets: a new approach to calculating crop ratios. *Archaeol. Anthropol. Sci.* 8, 29–42. <https://doi.org/10.1007/s12520-014-0190-7>.
- Weisskopf, A., 2017. A wet and dry story: distinguishing rice and millet arable systems using phytoliths. *Veg. Hist. Archaeobotany* 26, 99–109. <https://doi.org/10.1007/s00334-016-0593-8>.
- Wen, C.H., Lu, H.Y., Zuo, X.X., et al., 2018. Advance of research on modern soil phytolith. *Sci. China Earth Sci.* 61, 1169–1182. <https://doi.org/10.1007/s11430-017-9220-8>.
- Xiao, X.Y., Haberle, S.G., Li, Y.L., et al., 2018. Evidence of Holocene climatic change and human impact in northwestern Yunnan Province: High-resolution pollen and charcoal records from Chenghai Lake, southwestern China. *The Holocene* 28 (1), 127–139. <https://doi.org/10.1177/0959683617715692>.
- Xue, Y.N., Dal Martello, R., Qin, L., et al., 2022. Post-Neolithic broadening of agriculture in Yunnan, China: archaeobotanical evidence from Haimenkou. *Archaeol. Res. Asia* 30, 100364. <https://doi.org/10.1016/j.ara.2022.100364>.
- Yao, A., 2010. Recent developments in the archaeology of southwestern China. *J. Archaeol. Res.* 18, 203–239. <https://doi.org/10.1007/s10814-010-9037-7>.
- Zhang, E.L., Wang, Y.B., Sun, W.W., et al., 2016. Holocene Asian monsoon evolution revealed by a pollen record from an alpine lake on the southeastern margin of the Qinghai-Tibetan Plateau, China. *Climate of the Past* 12 (2), 415–427. <https://doi.org/10.5194/cp-12-415-2016>.
- Zhang, J.P., Lu, H.Y., Wu, N.Q., et al., 2010. Phytolith evidence for rice cultivation and spread in Mid-Late Neolithic archaeological sites in central North China. *Boreas* 39 (3), 592–602. <https://doi.org/10.1111/j.1502-3885.2010.00145.x>.
- Zhang, J.P., Jiang, L.P., Yu, L.P., et al., 2024. Rice's trajectory from wild to domesticated in East Asia. *Science* 384 (6698), 901–906. <https://doi.org/10.1126/science.adc4487>.
- Zhang, X.S., Liu, J.B., Rühland, K.M., et al., 2023. Concurrent mid-Holocene East Asian temperature and summer monsoon maxima forced by high-and low-latitude interplay. *Global Planet. Change* 220, 104008. <https://doi.org/10.1016/j.gloplacha.2022.104008>.
- Zhang, N.M., Dong, G.H., Yang, X.Y., et al., 2017. Diet reconstructed from an analysis of plant microfossils in human dental calculus from the Bronze Age site of Shilinggang, southwestern China. *J. Archaeol. Sci.* 83, 41–48. <https://doi.org/10.1016/j.jas.2017.06.010>.
- Zhao, Z.J., Chen, J., 2011. Flootation results and analysis of the Yingpanshan Site in Maoxian, Sichuan Province. *Southern Cultural Relics* (03).
- Zhang, X., Zheng, Z., Huang, K.Y., et al., 2020. Sensitivity of altitudinal vegetation in southwest China to changes in the Indian summer monsoon during the past 68000 years. *Quat. Sci. Rev.* 239, 106359. <https://doi.org/10.1016/j.quascirev.2020.106359>.
- Zuo, X.X., Lu, H.Y., Jiang, L.P., et al., 2017. Dating rice remains through phytolith carbon-14 study reveals domestication at the beginning of the Holocene. *PANS* 114 (25), 6486–6491. <https://doi.org/10.1073/pnas.1704304114>.